Appl. Phys. B 78, 111–117 (2004)
DOI: 10.1007/s00340-003-1282-8

Applied Physics B
Lasers and Optics

R. STEVENS
P. EWART✉

Single-shot measurement of temperature and pressure using laser-induced thermal gratings with a long probe pulse

Clarendon Laboratory, University of Oxford, Parks Road, Oxford, OX1 3PU, UK

Received: 3 July 2003
Published online: 8 October 2003 •

ABSTRACT We report accurate and precise single-shot measurements of temperature and pressure using laser-induced thermal grating spectroscopy (LITGS). The use of a flashlamp-pumped dye laser (FLPDL) as a probe for the induced gratings is described and a fast method of data analysis using Fourier methods is reported. Thermal gratings were induced by 8 ns pump pulses from a frequency-doubled Nd:YAG laser. The signals were produced by scattering 2-μs-long pulses, of energy 200 mJ, from the FLPDL. LITGS signals were obtained from NO_2/N_2 mixtures at pressures in the range 1–40 bar and temperatures between ambient and 400 K. Temperature values were derived from the data with an accuracy of 0.42% and a single-shot precision of 0.16%. Pressure values were obtained with an accuracy of 5.7% and a precision of 1.4% limited by uncertainties in the gas kinetic parameters.

PACS 63.62.Cf; 82.33.Vx

1 Introduction

Laser-induced thermal grating spectroscopy (LITGS) has been widely used in studies of condensed matter [1]. Recently such gratings have been exploited for gas-phase diagnostics. These gratings arise from the spatial modulation of the refractive index induced by two interfering laser beams. There are, in general, two contributions to such gratings. Firstly, a spatially periodic density variation is induced by local heating following absorption in the regions of constructive interference, and secondly, electrostriction occurs in these high-field regions. The gratings are conveniently detected by Bragg scattering of a third laser beam incident at the appropriate angle.

The absorption contribution is from a strongly resonant process and a stationary spatial modulation of temperature is established. The resultant density modulation initiates two counter-propagating acoustic waves that traverse the stationary temperature grating, leading to a periodic variation in the overall scattering efficiency. In resonantly absorbing gaseous media, scattering from this thermal grating usually dominates that from the nonresonant electrostrictive grating. In weakly absorbing gases, or in a nonresonant interaction, scattering from the electrostrictive grating may be comparable to, or exceed, that from the thermal grating. When the grating is induced by laser pulses of duration much shorter than the medium relaxation times, the stationary thermal grating and the associated acoustic waves lead to a time-dependent Bragg diffraction that oscillates and decays at a rate determined by the thermodynamic properties of the gas.

The potential of LITGS, or laser-induced thermal acoustics (LITA), for gas-phase diagnostics has been demonstrated by their use to measure temperature [2], gas dynamic properties [3], trace species concentrations [4, 5], temperature and pressure of high pressure flames [6], as well as bulk gas velocity [7]. In most demonstrations the thermal grating is induced by a pulsed laser with a pulse duration on the scale of nanoseconds, and the signal is produced by Bragg scattering of a cw probe laser. Typical situations involve a cw argon ion laser with a power of 1 W probing a grating with a lifetime on the order of 1 μs. This restricts the energy that can interact with the grating to 1 μJ and limits the achievable signal and signal-to-noise ratio. Nonetheless, concentrations on the scale of ppb have been detected under favourable circumstances [2]. A dramatic increase in sensitivity is expected if a pulsed high-power probe is used. Sampling of an electrostrictive grating has been achieved using a short-pulse probe recycled in a resonant cavity [8]. An alternative method has used a pulsed probe with a variable delay to plot the intensity of the scattered signal pulse as a function of delay time [9]. The first method is experimentally difficult and the second cannot be used for single-pulse or time-resolved measurements.

An elegant solution has been demonstrated using a pulse-stretched single-longitudinal-mode Alexandrite laser to provide a long-pulse probe [10, 11]. This rather complex and expensive system uses active control of the Q-switch pulse development to produce a long pulse on the order of microseconds whilst suppressing relaxation oscillations; single-mode operation is required to suppress mode beating.

In this paper the use of a relatively inexpensive flashlamp-pumped dye laser (FLPDL) to perform long-pulse probing of thermal gratings induced by a Q-switched Nd:YAG laser is reported. The flashlamp-pumped dye laser provides high-energy pulses on a time scale of a few microseconds with a smooth temporal profile.

✉ Fax: +44-1865/272400, E-mail: p.ewart1@physics.ox.ac.uk

The analysis of LITGS data is based on the solution of linearised hydrodynamic equations governing the evolution in time of the induced grating structure in the medium. The basic solution to these equations has been presented by Cummings [2] and by Paul et al. [12]. In general, analysis of experimental data by fitting to theoretical simulations based on these models is computationally expensive. Approximate methods providing rapid analysis by use of neural networks [13] or frequency analysis (using Pronys method) have been demonstrated. Neither the neural network approach nor Pronys method have been used to derive pressure from the LITGS signals. Approximate solutions in the time domain have been used which do not distinguish the details of the quenching processes [14]. (*Note added in proof.* At the proof stage the attention of the authors was drawn to an article by Hemmerling and Kozlov [15]. In this article a more detailed, although still approximate, analytical quenching model treating the particular case of LITGS in pure O_2 is presented. Within this approximation several distinct quenching processes, having relaxation times significantly different from the acoustic transit time, may be included in the model. Adjustment of quenching parameters yields fits to experimental data involving both thermal and electrostrictive gratings.)

Approximate solutions in the time domain have been used that do not distinguish the details of the quenching processes [8] and rapid analysis by use of neural networks [13] or frequency analysis (using the Pronys method) have been demonstrated. Both the Pronys method and the neural network approach have not been used to derive the pressure from the LITGS signals.

The second purpose of the present work is to report an alternative analysis procedure, which is sensitive to the details of the quenching mechanisms involved. Our approach is based on Fourier transform methods to provide accurate and precise measurements of both temperature and pressure from the experimental LITGS data.

This paper begins by outlining the theoretical basis for the analysis of LITGS signals and presents our alternative procedure for the rapid and accurate derivation of both temperature and pressure from experimental data. The generation of a suitable long-pulsed probe using a flashlamp-pumped dye laser is described, together with the experimental apparatus and procedure. The data obtained and the derivation of temperature and pressure values is then presented and the accuracy and precision of the measurements is discussed.

2 LITGS theory and analysis

The basic theory of LITGS has been presented by Cummings [2] and by Paul et al. [12], and is based on a model in which thermal gratings are created by collisional quenching of electronically excited states. Linearised hydrodynamic equations are used to describe the normalized perturbations in density, velocity, and pressure. The perturbations in these parameters lead to a solution consisting of two terms. The first corresponds physically to the stationary thermal grating that decays by thermal diffusion. The second corresponds to the two counter-propagating acoustic waves that set up a standing-wave acoustic grating that decays by viscous damping. The scattering efficiency of the combined grating structures thus oscillates as the acoustic waves traverse the stationary density grating induced by the temperature variation. Measuring the period of this oscillation for a known grating spacing, Λ, yields a measurement of the local sound speed, c. When the gas composition, and hence the gas dynamic properties, is known, this measurement of the local sound speed yields the gas temperature. The overall decay rate and that of the amplitude of the oscillations is determined by the gas viscosity, conductivity, and diffusivity. Thus, when the gas dynamic properties are known, the measured decay rates may be used to derive the gas pressure.

Analytic solutions in the time domain using the models of Cummings [2] and Paul et al. [12] are possible providing two simplifying conditions are met. Firstly, the grating must be created in a time very much shorter than the period of acoustic oscillations, τ, typically on the order of tens of nanoseconds; secondly, that the Reynolds number, $\mathrm{Re} \gg 1$. In general, the solution comprises two parts: a quickly varying 'acoustic grating' component, and a slowly varying 'thermal grating'. In practice, it is usually easy to satisfy the condition of large Reynolds number. However, rapid creation/formation of a grating is much more difficult. Several components of the source function for the grating evolve on time scales on the order of, or greater than, τ. The quenching time constant for the molecular excited-state population (which determines the heating rate for the thermal grating) may be on the order of 100 ns. Furthermore, the optical pulse used to create the grating is usually derived from a Q-switched laser, which can have a pulse duration on the order of τ. In such situations a numerical solution is required. The differing time scales involved constitute a stiff problem both from the physical nature of the processes and from the difficulty of finding a solution.

The overall source function, that is, the function describing the generation of the grating, must be evaluated by a convolution of the functions describing each component. The source function must then be convolved with the grating decay function. Convolutions with an arbitrary function must, in general, be evaluated numerically. Stiff problems require large arrays of closely spaced points to generate sufficient bandwidth for modelling. The time taken to convolve large arrays typically scales with $\sim N^2$ for an N-datapoint array, or with $N \log(N)$ for a Fourier domain evaluation, which is faster and more elegant. This cost is incurred for each element of the source function, and the cumulative cost can be excessive when the calculation is part of an iterative numerical fit to experimental data. Fitting routines often require, or work better with, expressions for the derivative of the variables in the minimisation (Jacobian matrix) and the matrix of covariances (Hessian matrix), which can also be costly to evaluate in a numerical computation.

2.1 *Fourier domain LITGS analysis*

The following analysis is based on the full theory developed by Paul et al. [12], in which the solution to the linearised hydrodynamic equations is found by declaring the problem to be irrotational, and to have a separable source function. The parameters of the problem are scaled in space by the grating spacing, Λ, and in time by τ. The normalised time,

ζ, and space, ξ, variables are therefore

$$\zeta = \frac{t}{\tau}\,; \quad \xi = \frac{x}{\Lambda}\,. \tag{1}$$

The problem is solved by a Fourier transform in space and a Laplace transform in time. The solution in 1-D space for a grating of dimensions $\gg c\tau$ is simply cosinusoidal. The Laplace transform solution for the separated time dependence is given by

$$\mathcal{R}(s) = \left\{ s^3 + \left[\frac{4(2\pi)}{3\,\mathrm{Re}} + \frac{(2\pi)^2}{\mathrm{Re\,Pr}} \right] s^2 + \left[(2\pi)^2 + \frac{4(2\pi)^4\gamma}{3\,\mathrm{Re}^2\,\mathrm{Pr}} \right] s + \frac{(2\pi)^4\gamma}{3\,\mathrm{Re\,Pr}} \right\}^{-1}, \tag{2}$$

where Pr is the Prandtl number of the gas, γ is the isentropic exponent, and s is the Laplace transform variable. In what follows the implications of solving this problem using the Fourier transform for both space and time dimensions are considered.

In general, solution of a differential equation by Fourier or Laplace methods results in quite different solutions, dependent on the position of zeros and poles in the complex plane. In the case of the time dependence of the density perturbation for a delta-function source at time $\zeta = 0$, it can, however, be shown that the solutions are identical. The Fourier, $\mathcal{F}$, and Laplace, $\mathcal{L}$, transforms for this work are defined respectively as

$$\mathcal{F}\{g(\zeta)\} = \int_{-\infty}^{\infty} g(\zeta)\,\mathrm{e}^{2\pi i\omega\zeta}\,\mathrm{d}\zeta = G(\omega), \tag{3}$$

$$\mathcal{L}\{g(\zeta)\} = \int_{0}^{\infty} g(\zeta)\,\mathrm{e}^{-2\pi s\zeta}\,\mathrm{d}\zeta = G(s), \tag{4}$$

where ω is the angular frequency. It may be observed that the solution for the density perturbation in the time domain, $\varrho(\zeta)$, has the property $\varrho(\zeta) = 0$ for all $\zeta < 0$. Thus the different limits on the integrals are made effectively equal, and we can exchange transforms with the substitution $s = -\mathrm{i}\omega$. Hence the Fourier transform of the grating time dependence is given by

$$\mathcal{R}(\omega) = \left\{ \mathrm{i}\omega^3 - \left[\frac{4(2\pi)}{3\,\mathrm{Re}} + \frac{(2\pi)^2}{\mathrm{Re\,Pr}} \right] \omega^2 - \left[(2\pi)^2 + \frac{4(2\pi)^4\gamma}{3\,\mathrm{Re}^2\,\mathrm{Pr}} \right] \mathrm{i}\omega + \frac{(2\pi)^4\gamma}{3\,\mathrm{Re\,Pr}} \right\}^{-1}. \tag{5}$$

The analytic forms for the quenching source function may be taken to be convolutions of decaying exponentials in time. A multi-step quenching process, $q(\zeta)$, can also be evaluated by the linear combination and convolution proposed by Paul et al. [12]; this holds its form when transformed to give $Q(\omega)$ – the exponential functions are simply replaced by Lorentzians. The form of the normalized quenching component, $q_n(\zeta)$, and its transform are given by

$$q_n(\zeta) = \frac{1}{\tau}\,\exp\left(-\frac{\zeta}{\lambda_n}\right), \tag{6}$$

$$Q_n(\omega) = \frac{1}{1 - 2\pi i\omega\lambda_n}, \tag{7}$$

where λ_n is the partial quenching rate of the n-th quenching branch. The transform does not affect the form of the linear combination, or the values of the branching frations ϵ_n, defined in [12]. The laser excitation pulse, $l(\zeta)$, for the grating is typically modelled using a Gaussian temporal profile, which is also trivial to Fourier transform analytically, giving $L(\omega)$. The normalized laser pulse (centered on $\zeta = 0$) and its transform are therefore

$$l(\zeta) = \frac{2\sqrt{\ln(2)}}{\tau_\mathrm{L}\sqrt{\pi}}\,\exp\left(-\frac{4\ln(2)\zeta^2}{\tau_\mathrm{L}^2}\right), \tag{8}$$

$$L(\omega) = \frac{2\sqrt{\ln(2)}}{\tau_\mathrm{L}}\,\exp\left(\frac{\pi\tau_\mathrm{L}^2\omega^2}{4\ln(2)}\right), \tag{9}$$

where τ_L is the FWHM of the excitation laser pulse.

The final expression for the time dependence of the density perturbation under Fourier transform, $\mathcal{Z}(\omega)$, is simply the product of the elements outlined here:

$$\mathcal{Z}(\omega) = \mathcal{R}(\omega)L(\omega)Q(\omega)\ldots\,. \tag{10}$$

This expression is readily differentiable for the Jacobian and Hessian matrix elements, which can significantly improve the efficiency and accuracy of fitting to experimental data. Fitting can be done either under Fourier transform (preferred), or the final function may be transformed into the time domain, where the results are presented more clearly. The principal advantage of this method is that there are efficient high-speed numerical routines (FFT, FFTW) available for transfer of either data or simulation both to and from the Fourier domain. This method is proposed and demonstrated here as a numerically fast and convenient way to analyse LITGS signals.

3 Experiment

3.1 *The Flashlamp-pumped dye laser (FLPDL)*

We have used a FLPDL to generate high-power pulses with durations of several microseconds with which to probe the thermal gratings induced by short (8 ns $\simeq 0.5\tau$) duration laser pulses. The FLPDL is particularly suited to the generation of long and temporally smooth pulses, since the short radiative lifetime of the dye prohibits the formation of relaxation oscillations characteristic of solid-state media such as ruby, Nd : YAG, and Alexandrite. Owing to the high gain of the dye amplifier, a long cavity with low finesse may be used, leading to ill-defined longitudinal modes, and so modulation by longitudinal mode beating is minimised.

FLPDLs are reasonably simple devices that are robust, reliable, and relatively inexpensive. However some features of such systems are potentially disadvantageous. Firstly, distortions of the beam profile and pointing instability are induced by thermal lensing during the flashlamp excitation. Beam distortions and unstable pointing lead to temporal variations in the coupling of the probe beam to the induced grating. Secondly, the inherently broad spectral bandwidth of the output is not well matched to the Bragg conditions, which demand a given wavelength to be incident at a particular angle for efficient scattering.

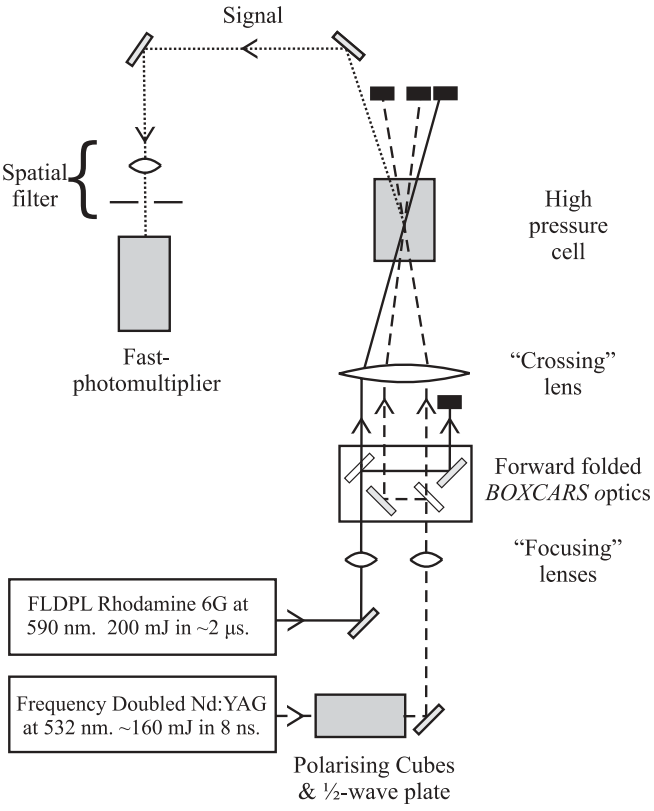

FIGURE 1 Experimental layout. See text for details

The present FLPDL system consisted of a modified Candela LDLF8 laser having a dye cuvette of length of 600 mm and diameter of 6 mm pumped in a diffuse reflective pumping chamber by a parallel linear flashlamp. Using Rhodamine 6G in methanol, pulses of up to 1 J energy with a duration of 3 μs were obtained at a repetition rate of 7 Hz.

In order to minimize the effects of thermal lensing the dye was dissolved in water instead of methanol and the solution maintained at 3.8 °C, at which the refractive index becomes independent of temperature. The usual plane parallel cavity was replaced by a confocal cavity comprised of a 3-m-radius-of-curvature high reflector and a plane output coupler in a cavity of length 1.15 m. An aperture was inserted near the output coupler to constrain the laser to TEM_{00} operation. These devices dramatically improved the beam uniformity and stability during the 2-μs pulses. The far-field beam profile was verified using a CCD camera to detect any beam distortion. The temporal stability was monitored by measuring the energy transmitted by a small aperture having the same transverse dimensions as the induced thermal grating. Finally the bandwidth was narrowed by an intra-cavity interference filter to a value of approximately 1 nm to more efficiently match the 1-nm (estimated) reflective bandwidth of the induced Bragg grating.

With the combination of water-based dye solutions held at around 4 °C, spectral narrowing, and restriction to TEM_{00} operation, the probe beam's coupling to the gratings was determined to be a reproducible, with a temporally smooth pulse with an energy of up to 200 mJ and 2-μs duration (FWHM). The experimental layout is shown in Fig. 1.

3.2 *Experimental procedure*

The capacity of an FLPDL for LITGS is demonstrated here using NO_2 in N_2 mixtures. NO_2 provides a suitable target species because (1) it exhibits absorption at the wavelength of a frequency-doubled Nd : YAG laser at 532 nm, (2) it is a stable species, (3) it is of interest in combustion diagnostics, and also, (4) it is an important atmospheric pollutant. Furthermore the quenching mechanism is known to be more than a simple single-stage process [14, 16], and so provides a more stringent test for the modelling of the LITGS dynamics. An NO_2/N_2 gas mixture was introduced into a high-pressure cell of length 50 mm and N_2 was added as a buffer gas to achieve pressures in the range 1–40 bar. The partial pressures of each gas were measured using a dial gauge (Schäfer and Budenberg) that had been calibrated to an accuracy of ±0.1 bar over the full range. A heating element was wound onto the exterior of the cell to allow variation of the temperature in the range 300–400 K, as measured by a thermocouple inserted into the wall of the cell.

The pump pulses used to excite the thermal gratings were derived from the output of a frequency-doubled Q-switched Nd : YAG laser (Spectron Lasers SL-404G) with a pulse duration of about 8 ns and an energy of typically 160 mJ. A system of polarizing prisms and a half-wave plate were used to reduce the total energy of the pump pulse to around 16 mJ for these experiments.

The pump beam was directed through a spherical "focusing" lens to a specially fabricated beam-splitting device producing two equal-intensity parallel beams with variable separation. The probe beam was also directed via a "focusing" lens to a similar beam splitter to produce two parallel probe beams. Both pump and both probe beams were aligned to propagate parallel to the axis of a 130-mm-focal-length "crossing" lens but in separate planes. This "crossing" lens was located with its front focal plane coincident with the back focal plane of the "focusing" lenses in the pump and probe beams. As a result the two pump and two probe beams crossed in the back focal plane of the "crossing" lens as parallel beams. This arrangement of defocussed forward folded-BOXCARS was previously introduced to optimize the signal-to-noise ratio in degenerate four-wave mixing experiments [17]. This arrangement also facilitates the direct adjustment of the separation of the two pump beams to determine the induced grating spacing. The position of the two probe beams was similarly adjusted to the correct angle for Bragg scattering from the grating. The signal beam arising from the scattering of the strong probe would then, by symmetry, emerge in the direction defined by the second probe. This second probe beam could be used to indicate the direction of the signal beam for detector alignment, but was blocked during the LITGS experiment. Once the beam positions were fixed, a calibration data set could be recorded under known conditions to determine the (constant) grating spacing for the experiment.

The gratings induced by the pump beams had a diameter of 4 mm ($\gg c\tau$), and the probe beam diameter was constrained to be less than the grating diameter to ensure reliable interaction from shot to shot. LITGS signals scattered from the grating in the high-pressure cell were directed via a spatial filter to a fast photomultiplier detector (Electron Tubes 9783B). The result-

ing signal was recorded on a digital oscilloscope (Tektronix TDS 3052 series, 500 MHz and 5 Gs/s). A small portion of the FLPDL pulse energy was recorded on a fast vacuum photodiode (Instrument Technology Ltd). Thus the temporal profile of both the incident probe pulse and the scattered LITGS signal were recorded simultaneously on each laser shot. The intensity profile of the probe was then used to normalize the recorded LITGS signal. The detectors were chosen to be able to respond to the fastest variation in the incident and scattered signals, but also to record signals reliably over a longer time scale. The acoustic oscillations were on a time scale of ~ 15 ns, whereas the overall signal decayed on a microsecond time scale. Fast detectors often display a distortion at low frequencies. In the present case effects arising from detection of transients occurring on widely different time scales contributed errors at the level of 2%. This error was eliminated by deriving an analytical instrument response function for both detectors that could be calibrated.

4 Results and analysis

Single-shot LITGS signals were recorded over a pressure range of 1–40 bar and with temperatures in the range 300–400 K. The temperature range was restricted by the properties of the rubber gaskets on the windows sealing the high-pressure cell. All the signals could be characterised by thermal gratings – no contribution from electrostrictive was evident in any of the data. A typical single-shot signal for NO_2 in N_2 at 5.44 bar is shown in Fig. 2a together with a theoretical fit to the data. Also shown is the smooth temporal profile of the FLPDL probe recorded simultaneously and used in the simulation fitting procedure. Of particular note is the high signal-to-noise ratio in the data and the excellent fitting by the simulation, as indicated by the residual of 2.2% in this case. Note that at around 5 bar the LITGS signal has decayed well within the probe pulse duration. Figure 2b shows a typical result at around 40 bar, for which the decay of the signal is due largely to the decay of the probe pulse intensity.

The simulation of the LITGS signals and fitting to the experimental data was executed according to the procedure outlined in Sect. 2. In order to constrain the fitting procedure the values of temperature, T, and pressure, P, were used as fitting parameters rather than Pr, Re, and γ. Since many of the gas kinetic parameters are sensitive to T and P, it was therefore necessary to evaluate them online since not all values were allowed. The following methods were used to calculate the relevant parameters and their variation with T and P.

For density, the Lee–Kesler–Plöker equations (from Benedict–Webb–Rubin) [18, 19] were used with analytic forms for the estimation of the binary interaction coefficients [20] to an accuracy of 2%. The Chapman–Enskog theory [18, 19] was used (although it is not strictly valid for polar molecules) to calculate the viscosity by the method of Chung et al. for low P, and by the method of Lucas for high P to an accuracy of 4%. The thermal conductivity was estimated using a subroutine from CHEMKIN II [21, 22], although the value obtained could be in error by as much as 20% [23]. Empirical polynomial expressions were used to calculate C_P, C_V, and γ for NO_2 using data from the literature [18, 19]. Values of C_P, C_V, and γ for N_2 were interpolated from published data [24] to an accuracy of 1%.

Using this information the values of T and P could be found by fitting a theoretical simulation to an experimental data trace with 4000 points using combined preconditioned conjugate gradients (PCG) and Levenberg–Marquardt minimization schemes with an on-line calculation of the gas kinetic parameters. Fitting to a single-shot data trace and eval-

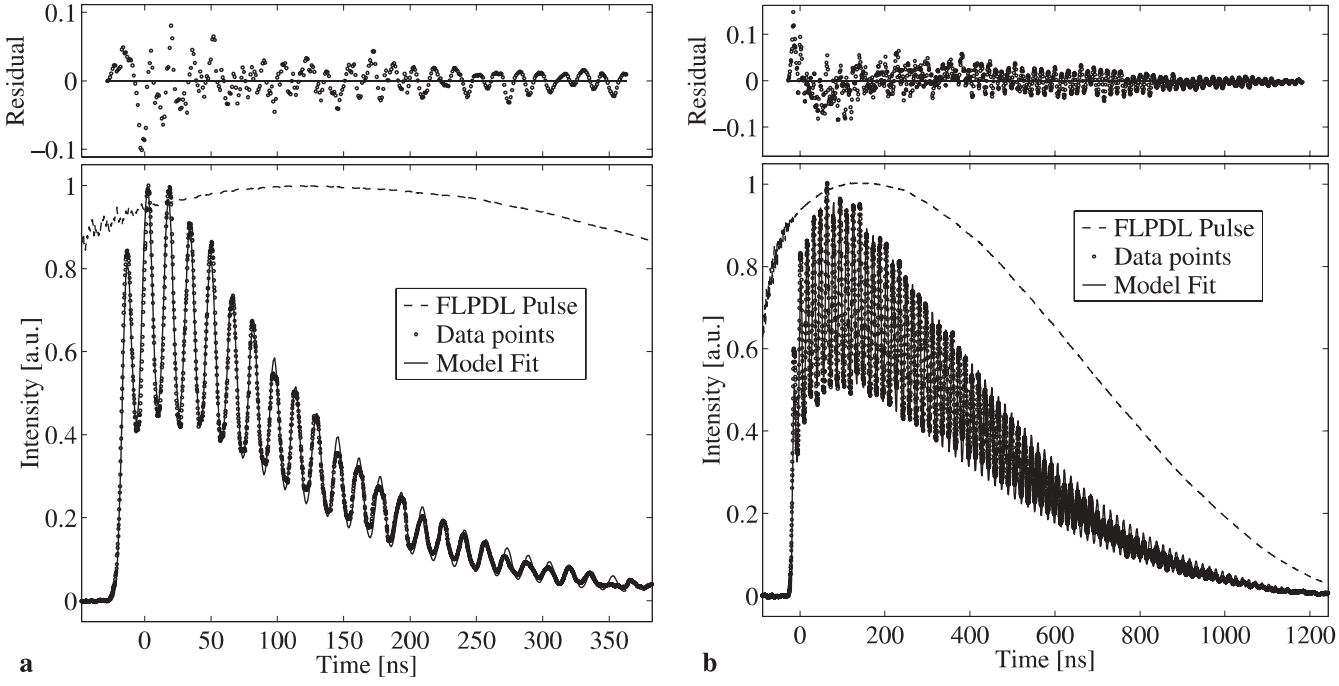

FIGURE 2 Typical single-shot LITGS signal in NO_2/N_2 with grating spacing $\Lambda = 5.556 \pm 0.005$ μm: **a** at 5.44 ± 0.07 bar with 5000 ppm NO_2 and a fit residual of 2.2%; **b** at 40.10 ± 0.07 bar with 625 ppm NO_2 and a fit residual of 2.5%

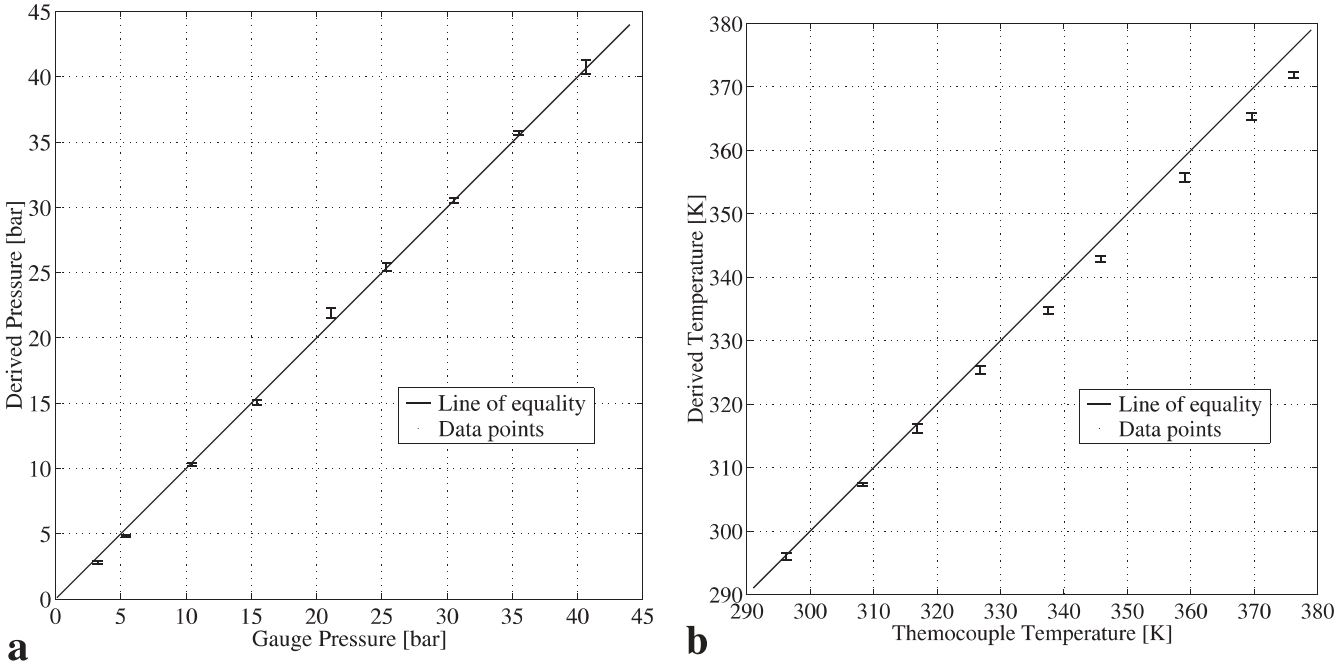

FIGURE 3 Single-shot derived pressure and temperature using an FLPDL for LITGS. In both plots each data point represents the average of 10 shots, with an error bar indicating the normalised standard deviation. **a** Derived pressure at 297 K: precision 1.4% and overall accuracy 5.7%. **b** Derived temperature at 10 bar: precision 0.16% and overall accuracy 0.42%

uation of T and P was accomplished in ~ 20 s using a PC with a 700-MHz Pentium III processor and 256 Mb of RAM. The fitting procedures displayed good convergence to a minimum but the speed and accuracy were limited by calculation of the gas kinetic parameters, a process which could be conducted using a fast lookup table if greater speed were required.

The accuracy of the experimental method and analysis was evaluated by comparing values of P and T derived from the LITGS data with those obtained from a dial gauge and thermocouple, respectively. For both P and T the accuracy was derived from two sets of ninety independent single-shot LITGS fits, spaced in nine sets of ten shots over the ranges specified, that is, 180 individual single-shots. Accuracy here is defined as the relative difference between the values derived from the LITGS data and the values indicated by the dial gauge or thermocouple. Specifically, the accuracy was calculated by evaluating the population standard deviation of the residuals about the line of equality shown in Fig. 3.

The precision was determined using the same ensemble of 180 single shots. The residuals were evaluated of each individual shot about the mean of ten data points at each temperature or pressure value. All the residuals were then used to evaluate the population standard deviation, which is quoted as the single-shot precision.

Single-shot measurements of P were made over the range 1–40 bar. The measurements were compared with the values determined by the 30-cm dial gauge (Schäfer and Budenberg) that had been previously calibrated against an absolute pressure testing machine. The results are shown in Fig. 3a, in which the precision of a single-shot measurement of 1.4% is indicated and the overall accuracy (limited by the uncertainties in gas kinetic data) was 5.7%. The LITGS measurements are shown to be accurate and precise over the entire range of pressures used in this work.

A similar test of accuracy and precision in the temperature measurement using LITGS is shown in Fig. 3b. The values derived from single-shot LITGS signals were compared with values obtained from a two-point calibrated K-type thermocouple (RS Components) inserted in the cell wall. The precision is shown to be 0.16% over the range 300–400 K with an accuracy of 0.42%. The data shows a tendency for the values derived from LITGS to fall slightly below the thermocouple value as T increases. This is most likely due to a real difference in temperature between the temperature of the wall and the gas in the interaction region at the centre of the cell. Unequal rates of heat loss from the windows relative to the insulated cell walls could easily account for such a difference.

As indicated in the discussion above, the overall accuracy of T and P values derived from LITGS signals is limited by the knowledge of thermodynamic parameters, which vary with both T and P and with gas composition. A second source of uncertainty is the dynamics of the quenching mechanisms involved in transferring absorbed energy to the thermal grating. For NO_2 we used a 2-stage quenching mechanism in which each stage has a markedly different relaxation rate. In general such slow and complex quenching mechanisms will be difficult to model accurately. Since quenching times decrease with increasing pressure, this problem is somewhat less serious at higher pressures. The accuracy of the analysis is improved as the quenching relaxation times tend to zero. Further improvement to the accuracy of the model would be obtained by including electrostrictive and other effects present to a small degree in the data presented here. These factors, however, result only in small corrections to the present

model and were omitted for simplicity and robustness in data analysis.

5 Conclusions

We have demonstrated the use of a flashlamp-pumped dye laser to make a long-pulse probe of LITGS signals in NO_2 mixtures in N_2 at pressures of up to 40 bar and temperatures of up to 400 K. The system provides a simple, relatively inexpensive method with the potential to increase the sensitivity of LITGS over conventional cw probes or expensive and complex solid-state systems. In addition we have reported a fast numerical procedure for the analysis of LITGS signals in terms of temperature, T, and pressure, P. Single-shot measurements of P were made with a precision of 1.4% and an accuracy of 5.7%, limited by uncertainties in estimating gas kinetic data. Similarly single-shot measurements of T were made with a precision of 0.16% and an accuracy of 0.42%.

The system highlights the potential of LITGS for temporally and spatially resolved measurements of P and T. Such measurements are of considerable utility for non-invasive diagnostics of gas-phase media. This technique may be applied to combustion, plasmas, shock-tube studies, or other situations for which measurements are required of these parameters in transient processes or hostile environments.

ACKNOWLEDGEMENTS The authors would like to thank Dr. P.H. Paul for his invaluable discussions on this topic, and Dr. C.R. Stone for the loan and calibration of the pressure dial gauge and thermocouples used. We thank Dr. D. Coutts for his discussion of the optical arrangement used here and Dr. A. McGonigle for his practical help and advice with the FLDPL. R. Stevens is grateful to the EPSRC for personal financial support.

REFERENCES

1 H.J. Eichler, P. Günter, D.W. Pohl: *Laser Induced Dynamic Gratings* (Springer Verlag, Berlin 1986)
2 E.B. Cummings: Opt. Lett. **19**, 1361 (1994)
3 E.B. Cummings, H.G. Hornung, M.S. Brown, P.A. Debarber: Opt. Lett. **20**, 1577 (1995)
4 A. Dreizler, T. Dreier, J. Wolfrum: Chem. Phys. Lett. **233**, 525 (1995)
5 B. Hemmerling, R. Bombach, W. Hubschmid: Chem. Phys. Lett. **256**, 71 (1996)
6 H. Latzel, A. Dreizler, T. Dreier, J. Heinze, M. Dillmann, W. Stricker, G.M. Lloyd, P. Ewart: Appl. Phys. B. **67**, 667 (1998)
7 D.J.W. Walker, R.B. Williams, P. Ewart: Opt. Lett. **23**, 1316 (1998)
8 B. Hemmerling, D.N. Kozlov: Appl. Opt. **38**, 1001 (1999)
9 E. Loubignac, B. Attal-Tretout, S. Le Boiteux, D. Kozlov: C.R. Acad. Sci. Ser. IV-Phys. Astrophys. **2**, 1013 (2001)
10 R.C. Hart, R.J. Balla, G.C. Herring: Appl. Opt. **38**, 577 (1999)
11 R.C. Hart, R.J. Balla, G.C. Herring: Appl. Opt. **40**, 965 (2001)
12 P.H. Paul, R.L. Farrow, P.M. Danehy: J. Opt. Soc. Am. B **12**, 384 (1995)
13 S. Schlamp, H.G. Hornung, E.B. Cummings: Meas. Sci. Technol. **11**, 784 (2000)
14 R. Fantoni, L. DeDominicis, M. Giorgi, R.B. Williams: Chem. Phys. Lett. **259**, 342 (1996)
15 B. Hemmerling, D.N. Kozlov: Chem. Phys. **291**(3), 213 (2003)
16 P.A. Delve, B.J. Whitaker: Phys. Chem. Chem. Phys. **2**, 5594 (2000)
17 A.J. Grant, P. Ewart, C.R. Stone: Appl. Phys. B **74**, 105 (2002)
18 R.C. Reid, J.M. Prausnitz, B.E. Poling: *The Properties of Gases and Liquids*, 4th edn. (McGraw-Hill, New York, London 1987)
19 B.E. Poling, R.C. Reid, J.M. Prausnitz, J.P. O'Connell: *The Properties of Gases and Liquids*, 5th edn. (McGraw-Hill, New York, London 2001)
20 S.D. Labinov, J.R. Sand: Int. J. Thermophys. **16**, 1393 (1995)
21 R.J. Kee, G. Dixon-Lewis, J. Warnatz, M.E. Coltrin, J.A. Miller: SAND86-8246 (Sandia National Laboratories, Livermore 1986)
22 R.J. Kee, F.M. Rupley, E. Meeks: SAND96-8216 or UC-405 (Sandia National Laboratories, Livermore 1996)
23 P.H. Paul: SAND98-8203 and UC-1409 (Sandia National Laboratories, Albuquerque, Livermore 1999)
24 N.B. Vargaftik, Y.K. Vinogradov, V.S. Yargin: *Handbook of Physical Properties of Liquids and Gases: Pure Substances and Mixtures*, 3rd augm. and revised edn. (Begell House, New York 1996)